Journal of Brilliant Engineering 1 (2026) 41062
Brilliant Engineering
journal home: www.acapublishing.com/journals/4/ben

Research Article

Computational Modeling of Cannabidiol and Δ⁹-Tetrahydrocannabinol Derivatives from the Thermal Degradation of Cannabis sativa

Micah O. Omare*[1,3], Joshua K. Kibet[2], Obed M. Nyabaro[1].
[1]Department of Chemistry, School of Pure and Applied Science, Kisii University, P.O Box 408 -40200, Kisii, Kenya
[2]Department of Chemistry, Egerton University, P.O Box 536-20115, Egerton, Kenya
[3]Africa Center of Excellence II in Phytochemicals, Textiles and Renewable Energy (ACE II PTRE), Moi University, Eldoret, P.O. Box 3900-30100, Eldoret, Kenya

Keywords

Theoretical and experimental,
Longitudinal dent number,
Hydrostatic pressure,
Cylindrical shell,
CFRP strips.

Abstract

Cannabis sativa is an intricate plant biomass that comprises over 400 chemicals, including at least 61 cannabinoids that undergo pyrolytic degradation during smoking, generating thousands more than 2000 chemical compounds with potential toxicological effects. Despite widespread use, the mechanistic pathways of cannabinoid decomposition, particularly for Δ⁹-tetrahydrocannabinol (Δ⁹-THC) and cannabidiol (CBD), remain poorly understood. This study investigates the thermal degradation of Δ⁹-THC and CBD, with a focus on their electronic structures, stability, and potential toxic byproducts. Computational modeling was performed using Gaussian 09 at the density functional theory (DFT) level with the B3LYP/6-311G++ basis set to evaluate molecular orbital behavior and energetics. Toxicity estimations of degradation products were carried out using the HyperChem platform. CBD was found to decompose into reactive species such as α-terpinyl radical, limonene, and olivetol, which are associated with oxidative stress and carcinogenic potential. The geometry optimizations converged after 40 (CBD) and 68 (THC) steps, with energies stabilizing at −968.519 and −968.727 Hartrees, respectively. Frontier molecular orbital analysis showed Δ⁹-THC has a wider HOMO-LUMO band gap than CBD, suggesting greater electronic stability. Solubility modeling revealed CBD is markedly more soluble in octanol than in water compared to its radical derivatives, while degradation byproducts displayed elevated toxicity indices. Computational evidence indicates that CBD thermal degradation produces toxic radicals with significant biological risks, including oxidative stress and impaired pulmonary function. These findings provide novel insight into cannabinoid pyrolysis pathways and highlight the need for experimental validation to better understand their health impacts in humans.

1. Introduction

Marijuana, scientifically termed Cannabis sativa, is second only to tobacco as the most widely abused illicit recreational substance worldwide [1]. The rising trends in misuse are associated with the ratification and acceptance of cannabis use in some nations, like Canada and several states in the United States of America, thus making it easily accessible [2]. Cannabis is a chemically complex plant material comprising more than 500 identified compounds, including approximately 60 cannabinoids [3]. When combusted, it thermally degrades to yield more than 2000 toxic and nontoxic compounds [4, 5]. Consumers are addicted to cannabis smoking due to the high concentration of the principal psychotropic cannabinoid, Δ⁹-THC, shown as (a) in Figure 1, which excites the smokers' brain, thus altering memory, movement, mood, perception, and cognitive dysfunction [6, 7]. Moreover, Δ⁹-THC stimulates dopamine release and euphoric sensations, which are accompanied by anxiolytic effects in users [8]. In addition, harmful psychological and physical effects characterized by psychiatric disorders and disruptive effects on the pulmonary and respiratory systems are associated with uncontrolled cannabis use [2, 9].

Regardless of the potential negative effects of Cannabis, it finds applications in medicine to manage acute and prolonged pain. This has been attributed to the presece of CBD that has demonstrated promising health benefits, such as anticonvulsant, antioxidant, neuroprotective, and anti-inflammatory properties [10]. CBD, indicated as (b) in Figure 1, allosterically modulates CB2 receptors and subsequently reduces chronic body pain, seizure frequency, and cutaneous irritation in patients [2]. These potentials of cannabis have led to its incorporation in controlling drug-resistant epilepsy, psychosis, and post-traumatic stress complications [11]. Some of these pharmacological characteristics of marijuana are significantly contributed by more than 18 classes of chemical compounds, including terpenes that have toxicological variations in the defense offered by CBD [12-14]. These chemical compounds enter the smokers' body systems once a marijuana cigarette puff is made as part of mainstream smoke components and sometimes into non-smokers' systems by inhalation of sidestream smoke, where they induce disruptive and toxicological consequences on the pulmonary and respiratory systems [15].

Additionally, the toxicological profiles of the molecular compounds and their reactive intermediates generated by uncontrolled temperatures during the thermal degradation of biomass have become a subject of health and environmental concern [16]. Marijuana, like any other biomass material, releases a myriad of thermal degradation pollutants that cause medical complications such as oxidative stress, cancer, and acute respiratory, pulmonary, and bronchial infections, attracting significant attention in cannabis toxicity studies [17, 18]. Despite its known toxic effects, marijuana has been legalized for recreational and medicinal use in several countries, including Canada [19]. However, rising

*Corresponding Author: omarmitmicah@gmail.com
Received 18 Aug 2025; Revised 18 Sep 2025; Accepted 18 Sep 2025
https://doi.org/10.36937/ben.2026.41062

consumption rates among youths and adults, both in legalized and non-legalized regions, have raised significant public health concerns. This trend accentuates the need for further research into the toxicological mechanisms induced by cannabis smoke inhalation [20, 21].

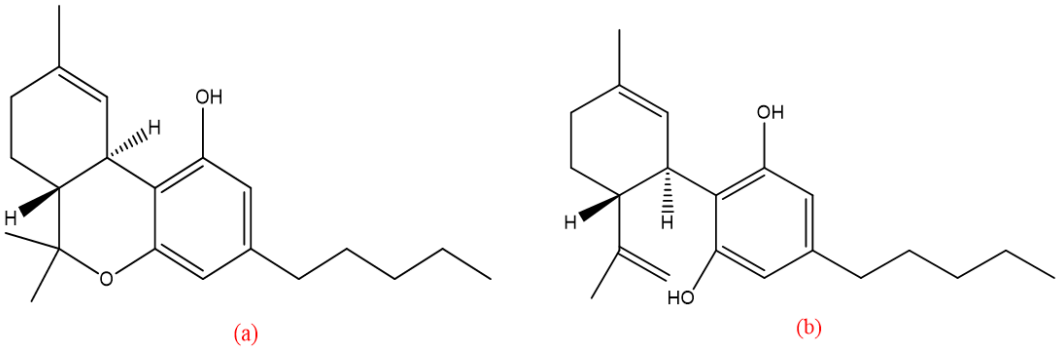

Figure 1. (a) Δ⁹-THC molecule structure and (b) CBD molecule structure

Computational chemistry tools can be viewed as reasonably cost- effective and time- efficient techniques that offer a better understanding of the molecular properties of a given chemical compound [22]. As a technique, computational modeling enhances the understanding of complex systems by manipulating variables that characterize a simulated system under study, generating results that help scientists predict what occurs in a real system [23]. Notably, the literature on the mechanistic thermal degradation of cannabis cannabinoids, particularly Δ⁹-THC and CBD, is limited. Therefore, this study employed a computational approach to investigate the thermodynamic stability, electronic structure, and mechanistic pathways of cannabis derivatives from the thermal degradation of marijuana. In addition, the toxicity profiles of the selected cannabinoid derivatives have a paucity of data on structure-activity relationships regarding their pyrolysis.

2. Computational Methodology

Electronic structure Calculations: The theoretical and electronic DFT calculations of the molecules under investigation were performed using the Gaussian 09 quantum chemistry package, as detailed by Kibet, Mathenge, Limo and Omare (24) and Tomberg (25). The B3LYP hybrid function level and 6-311G++ basis set with diffuse and polarized functions for enhanced accuracy in modelling delocalized electrons and radical species were employed in conducting calculations according to.

Geometry optimization: The initial structures of Δ⁹-THC and CBD were optimized to their global minima using the default Gaussian threshold convergence criteria at a root mean square force of <0.0003 hartree/Å. The point of the true energy minima was confirmed by vibrational frequency analysis [25].

Thermodynamic properties: Single-point energy calculations of the gaseous state molecules of Δ⁹-THC and CBD were performed at temperature increments of 50 K, ranging from 623 K -1023 K and a pressure of 1 atmosphere under conditions simulating smoking. The enthalpy changes of formation for degradation products, such as free radicals from CBD, was calculated using Eq. (1), the formalism of Mosoniket al (22);

$$\Delta_r H^\circ = \sum(\varepsilon_0 - H_{corr})_{products} - \sum(\varepsilon_0 - H_{corr})_{Reactants} \quad (1)$$

where $\Delta_r H^\circ$ is the variation in reaction enthalpy, H_{corr} is the enthalpic correction term, and ε_0 is the summation of electronic and thermal enthalpy terms.

Electronic structure analysis: Frontier orbital set (HOMO/ LUMO) together with contours were analyzed to assess and predict the reactivity of the molecules through band gaps and nucleophilic or electrophilic sites. In addition, electrostatic potential surfaces were generated to visualize the charge distribution and radical stabilization [26].

Toxicity estimation; HyperChem 8.0 (Hypercube, Inc.) with Quantity Structural Activity Relationship (QSAR)-based models were used to estimate the toxicological profiles of Δ⁹-THC and CBD, together with their subsequent radicals [27].

3. Results and Discussion

3.1. CBD thermal degradation mechanistic pathway

The thermally initiated degradation of cannabis most likely results in the release of numerous particulate matters, some of which have attracted considerable concern regarding public health. Accordingly, long-chain hydrocarbon compounds, aromatic hydrocarbons, and persistent free radicals, which are notoriously known for their carcinogenic potential, reactive oxidative stress, and pulmonary and respiratory system performance inhibition, are generated during the thermal degradation process as by-products [28].

The thermal degradation of CBD possibly starts by thermally breaking down, leading to the formation of two reactive radicals: 2,6-dihydroxy-4-pentylbenzene-1-yliumyl (CBD hydroquinone) radical and 3-methyl-6-(prop-1-en-2-yl) cyclohex-2-en-1-yliumyl radical, as suggested in Figure 2. Consequently, these free radicals react with hydrogen atom donors (antioxidants), as indicated in steps 2 and 3 in the above scheme, resulting in the formation of stable non-radical molecules, 5-pentylbenzene-1,3-diol and 1-methyl-4-(prop-1-en-2-yl) cyclohex-1-ene, respectively.

From the thermal degradation mechanistic pathway described in Scheme 1, it is evident that can be converted to radicals that have been classified as environmentally persistent free radicals with a long lifespan and are well-established biological pollutants [29]. For this reason, these cannabinoid derivatives can potentially react with human body cells, including lipids and microsomes, causing severe cellular destruction and consequently oxidative stress and malignant cells [28, 30]. For instance, 3-methyl-6-(prop-1-en-2-yl) cyclohex-2-en-1-yliumyl is a carbocationic radical which is a highly reactive intermediate [31]. It is a terpenoid-derived allylic carbocation, a group of compounds that have been reported to possess high antiparkinsonian activity [32]. This compound is highly electrophilic and has the potential to cause deleterious

damage to biological cells by attacking DNA, lipids, and body proteins and initiating mutagenesis, cytotoxicity, lipid peroxidation, and enzyme inactivation [32-35].

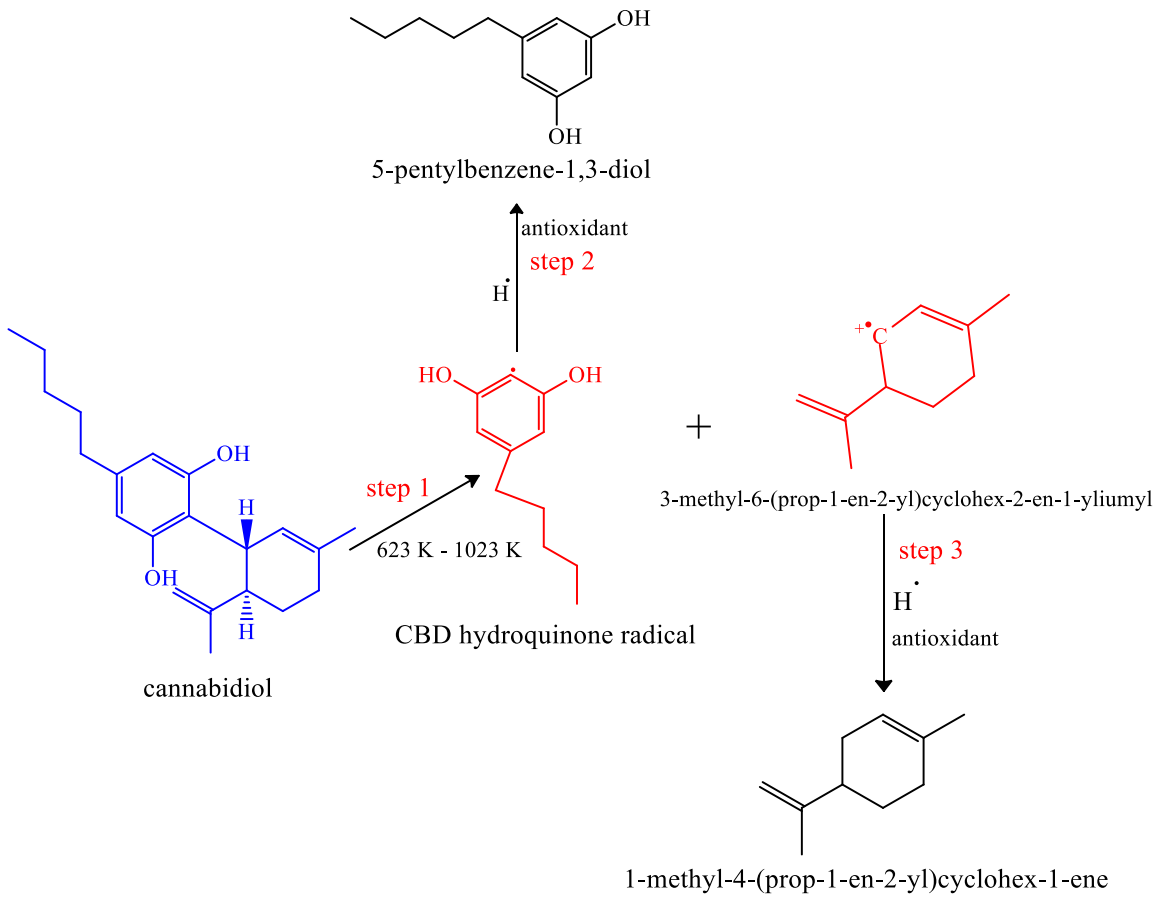

Figure 2. Proposed mechanistic pathways for thermal degradation of CBD

In contrast, the resulting stable monoterpene compound, 1-methyl-4-(prop-1-en-2-yl) cyclohex-1-ene (commonly known as limonene), is obtained from the hydrogenation of 3-methyl-6-(prop-1-en-2-yl) cyclohex-2-en-1-yliumyl radical. Limonene has been acknowledged as a probable renal toxicant, since it has been shown to induce hyaline droplet nephropathy and renal tubular tumorigenesis in rats, leading to toxicological concerns regarding chronic exposure in humans [36].

Nonetheless, 5-pentylbenzene-1,3-diol (commonly known as olivetol) is not regarded as a toxicant following oral ingesting. However, it is associated with adverse effects, including ocular irritation and damage, dermal inflammation (with exacerbation of pre-existing dermatitis), and respiratory tract irritation [37]. Furthermore, it is a suspected carcinogen due to potential long-term respiratory system exposure [38].

3.2. Δ⁹-THC thermal degradation mechanistic pathway

Upon thermal degradation, cannabis generates hazardous combustion byproducts via chemical reactions that involve the conversion of Δ⁹-THC into numerous chemical compounds in various steps at different temperatures, as proposed in Figure 3.

The primary degradation route encompasses the oxidation of Δ⁹-THC to a more stable and aromatic cannabinol (CBN), as illustrated in step I at temperatures of approximately 423–473 K [39]. This oxidation step involves the conjugation of the aromatic ring by oxidizing the resorcinol ring with a methyl group, followed by dehydrogenation and rearrangement to form CBN [40]. The formed CBN is less psychoactive than Δ⁹-THC [41]. As the temperature increases above 473 K, the reactions are subsequently followed by a series of ring opening and fragmentations that include the terpene moiety cleavage leading to the formation of small volatile hydrocarbons such as isoprene, acetone, methanol, toluene, and benzene, as indicated in step II.

The oxidation of Δ⁹-THC and CBN at temperatures of 573 K leads to the formation of quinones, such as delta-8-THC- quinone (Δ8-THCQ), CBD-quinone (CBDQ), and benzoquinones, owing to the oxidation of the phenolic ring. The resulting quinones, Δ8-THCQ and CBDQ, have been reported as potential disruptive agents of ciliary dysfunction and cellular pathway irritants [42]. In addition, the thermolysis of the formed quinones at temperatures of 773 K and above leads to the pyro synthesis of toxic polycyclic aromatic hydrocarbons such as naphthalene, anthracene, and benzo [a] pyrene (BaP). For instance, BaP is a known cancer-causing agent and mutagen that is metabolically activated, causing oxidative stress and disruption of the endocrine system [43]. This is owed to the fact that benzo (a) pyrene is highly lipophilic and therefore readily gets into the smoker's body system through marijuana smoke inhalation [44]. However, naphthalene has been reported to be a possible carcinogen (group 2B) by the IARC [45]. Anthracene has not been reported or classified as a carcinogenic agent in humans, but its oxidized derivatives, such as 1-hydroxyanthracene, antraquinone, and anthrone, have mutagenic and carcinogenic effects [46, 47].

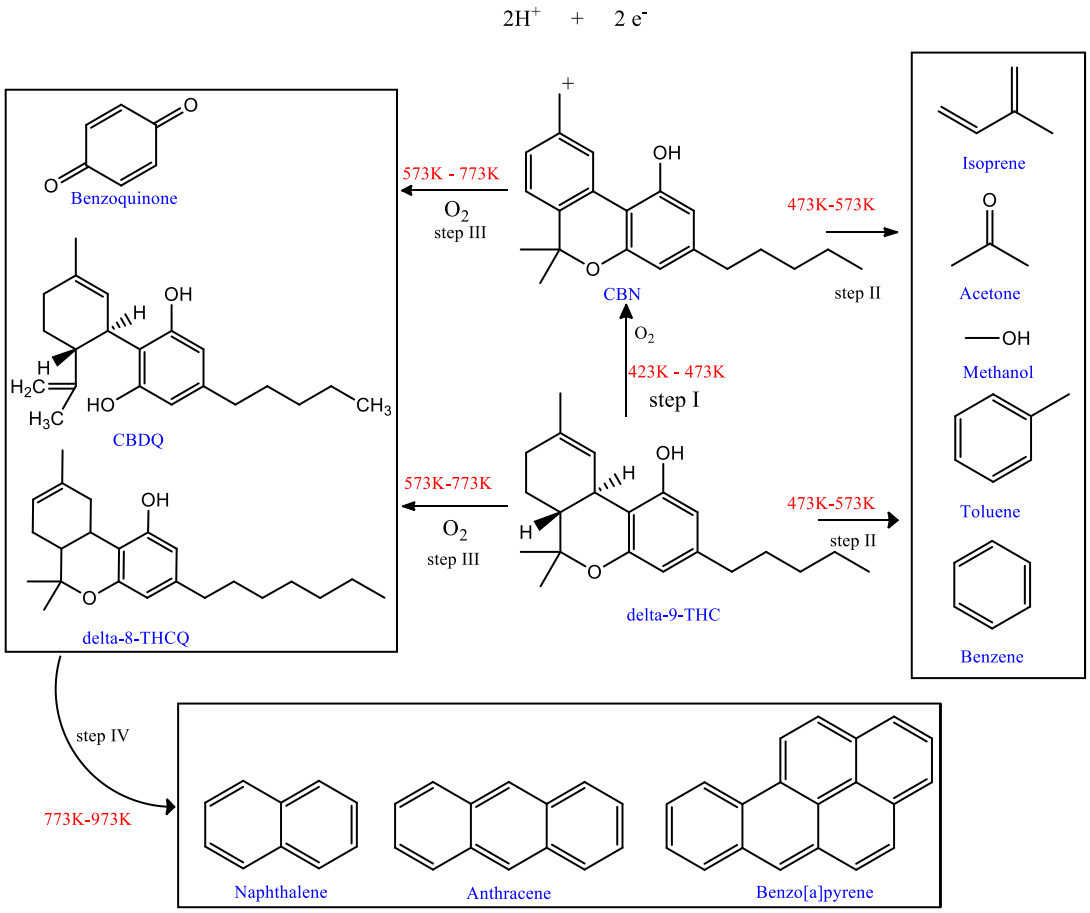

Figure 3. Thermal degradation mechanisms of Δ⁹-THC

3.3. Thermodynamic analysis

The energy change that occurs in the formation of subsequent radicals from the thermal degradation of CBD was computed using thermodynamic Eq. (1), and the corresponding results are presented in Table 1.

Table 1. Sum of electronic and thermal enthalpies of CBD

Temp (K)	3-methyl-6-(prop-1-en-2-yl) cyclohex-2-en-1-yliumyl radical (Hartree/particle)		2,6-dihydroxy-4-pentylbenzene-1-yliumyl radical (Hartree/Particle)		CBD (Hartree/Particle)	
	ε_0	H_{corr}	ε_0	H_{corr}	ε_0	H_{corr}
623	-389.903258	0.179111	-578.24437	0.181822	-968.95208	0.665138
673	-389.290654	0.171493	-577.53207	0.289704	-967.93814	0.591749
723	-389.67805	0.27147	-576.91946	0.285186	-967.92266	0.56136
773	-389.631467	0.327053	-576.8691	0.331775	-967.82767	0.69284
823	-389.670897	0.274623	-576.91181	0.291363	-967.90489	0.610075
873	-389.675227	0.278146	-576.84821	0.321354	-967.90653	0.57872
923	-389.649765	0.318755	-576.83805	0.323471	-967.90343	0.587125
973	-389.632792	0.311249	-576.89546	0.327429	-967.86587	0.6541
1023	-389.631471	0.311505	-576.88388	0.322176	-967.86074	0.627286

A plot of the enthalpy changes for the generation of CBD reactive intermediates displayed an exponential gradual rise, as shown in Figure 4. Notably, at low temperatures, CBD absorbs more heat energy that is required to break the carbon-carbon, carbon-oxygen, oxygen-hydrogen, and carbon-hydrogen bonds present in its structure; therefore, more energy is required for bond breaking. As the thermolysis reaction proceeds, temperature elevation consequently produces faster rates of degradation reactions. This results into higher kinetic energies of the absorbing atoms and eventually high system entropy. Consequently, less energy is required to break the remaining bonds, which may be the reason for

the slight decrease in the enthalpy changes at high temperatures. This suggests that the spontaneity of the CBD reaction increases with increasing temperature. Since under normal conditions of marijuana smoking, heating is involved, CBD is likely to be a highly reactive molecule with biosystems where it is prone to be disastrous.

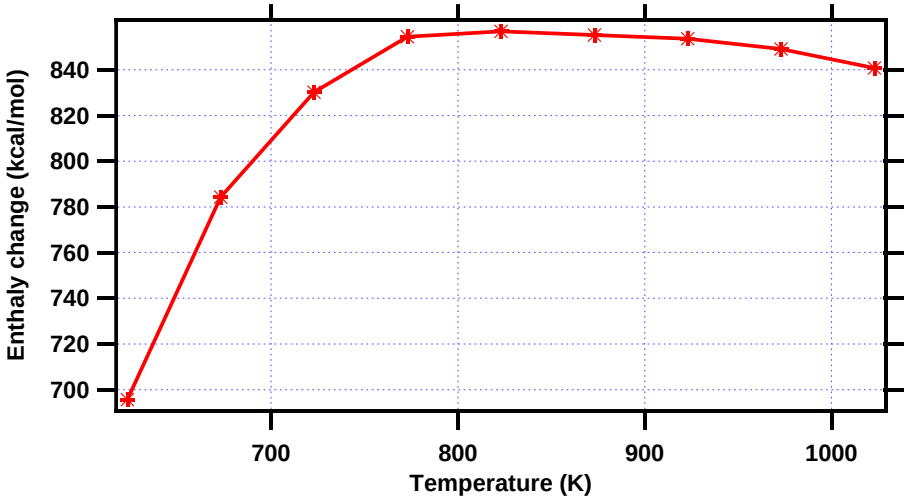

Figure 4, A graph of enthalpy of formation of radicals verses temperature

3.4. Molecular geometries of cannabis derivative

The configuration of a given molecule and the position of its building atoms are largely determined by geometric parameters, including bond angles, torsional angles, and bond lengths [48]. This investigation employed DFT with the B3LYP functional and the 6-311G++ basis set to examine the lowest-energy conformations of cannabidiol (CBD) and Δ⁹-tetrahydrocannabinol (Δ⁹-THC). Structural optimization was confirmed once the molecular potential energy surfaces reached their global minima, allowing for accurate predictions of thermodynamic behavior, spectroscopic characteristics, and reaction kinetics. With the help of Gaussian geometry-optimized structures, one can obtain the most stable structure of a molecule or compound of choice. Stable and optimized structures enable the estimation of factors that can block a reaction from occurring [49]. Therefore, one can develop a chemical reaction mechanism, which is crucial in forecasting and understanding the toxicity and reactivity of the compound under study [50]. During the structural optimization of CBD and Δ⁹-THC, the initial molecular configurations were subjected to iterative quantum mechanical calculations. These computations evaluated the electronic wave functions and system energies at each step, systematically converging toward the most stable molecular conformations with minimized potential energy.

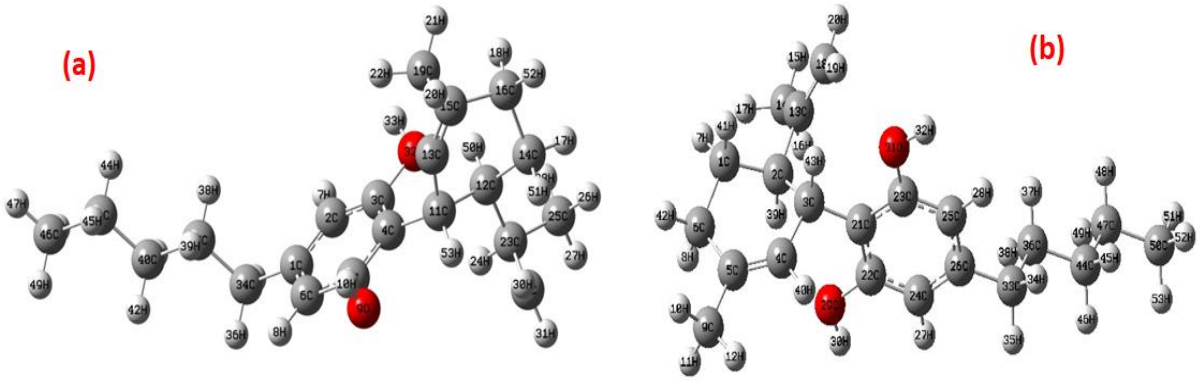

Figure 5. (a) initial CBD geometry (input structure) and (b) CBD final optimized geometry

The geometry optimization process for CBD required 40 iterative steps to reach convergence. The initial structure, with a calculated energy of -968.408 Hartree at step 0.924092, progressively stabilized until achieving the lowest-energy conformation at -968.519 Hartree upon completion at step 40. This energy minimization trajectory is illustrated in Figure 6.

In contrast, the optimization of Δ⁹-THC required 68 iterations, with the system energy decreasing from an initial -968.624 Hartree (step 1) to a final -968.727 Hartree (step 68). This process involved significantly more steps than that of CBD, reflecting greater conformational complexity. Arguably, the number of optimization steps reflects the computational effort required for a molecule to reach its energetically favored conformation. This information provides valuable insights into molecular stability, which can help anticipate its interactions and reactivity within biological environments [51]. Thermodynamically stable molecular conformations exhibit reduced chemical reactivity compared to their higher-energy counterparts when interacting with biological systems [52]. The computational analysis reveals distinct stability profiles between these cannabinoids. Δ⁹-THC's extended optimization trajectory (68 steps vs. CBD's 40) indicates greater conformational stability. This thermodynamic advantage suggests Δ⁹-THC may maintain structural integrity longer in biological systems, while CBD's relative instability could potentially lead to enhanced metabolic conversion rates, more reactive intermediate formation and greater tendency for off-target interactions.

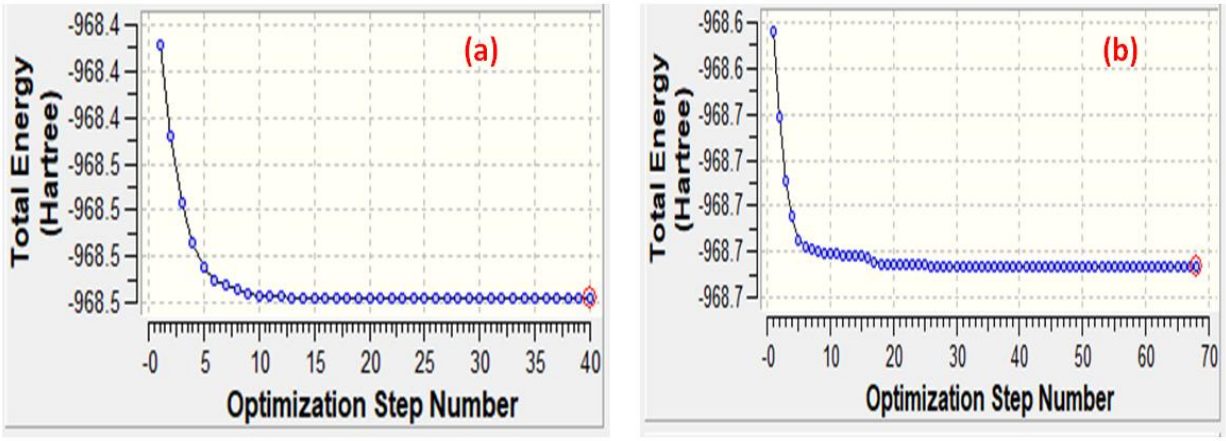

Figure 6. (a) CBD convergence plot and (b) Δ⁹-THC convergence plot

3.5. CBD molecular orbitals and electronic properties

Understanding a molecule's reactive behavior requires precise characterization of its electronic configuration [53]. In addition, frontier molecular orbital analysis proves particularly valuable for predicting sites of electrophilic/nucleophilic attack, estimating activation energy barriers and rationalizing preferred reaction pathways [54]. The spatial distribution and band gap energy between the HOMO and LUMO orbitals directly govern a compound's chemical susceptibility, redox potential and interaction selectivity with biological targets [55]. The HOMO and LUMO energy profiles for CBD and THC optimized geometry diagrams relating to their ionization potentials and electron affinities are presented in Figures 7 and 8, respectively. Notably, from Figure 5, it is evident that CBD has both alpha and beta molecular orbitals, with the HOMO in the range being orbital 86 at an energy of -0.340 eV in both. This was the highest energy attained, indicating that the orbital was slightly destabilized compared to the other orbitals. In contrast, the LUMO for both CBD alpha and beta was orbital number 87 at an energy of -0.183 eV. This resulted in HOMO-LUMO band gap energy of 0.157 eV.

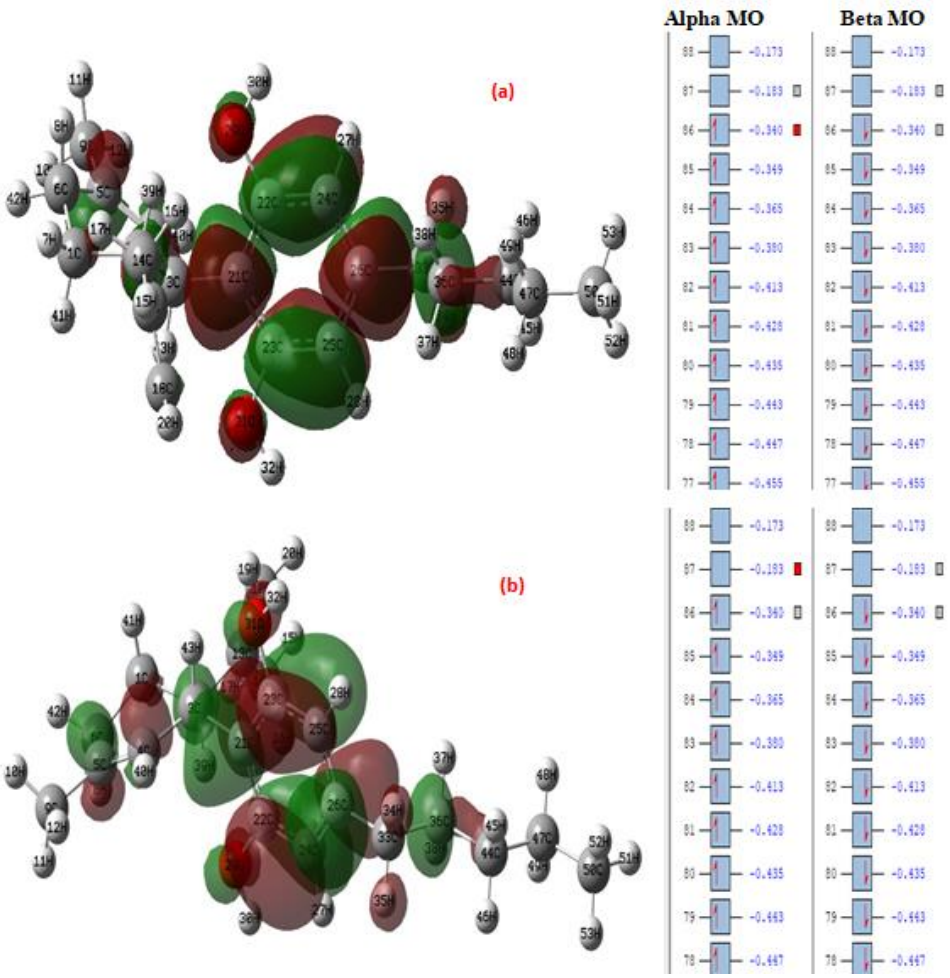

Figure 7. (a) CBD HOMO and (b) CBD LUMO

Accordingly, Δ⁹-THC displayed alpha molecular orbitals only, as indicated in Figure 6 below, with the HOMO and LUMO being orbital 86 and 87 at energies of 0.216 eV and -0.002 eV, respectively. This resulted to HOMO-LUMO band gap energy of 0.214 eV in Δ⁹-THC. The energies become increasingly negative with decrease in orbital number. For instance, in CBD, orbital 77 had the lowest energy at -0.455 eV. This implies that it had the greatest stabilization which is usually typical for lower energy orbitals closer to the bonding orbitals [56]. All the orbital energies were negative values, which is in agreement with bound state in quantum chemical calculations. It also confirms that our Gaussian 09 generated orbitals were stable since the more negative the value, the more stable the orbital is [57].

According to Janani, Rajagopal, Muthu, Aayisha and Raja (58), the band gap energies are important and mostly applied in describing the energy gap within the valence band and the conduction band in a compound or solid, and thereby they provide an understanding on how the band gap affects the electrical and chemical behavior of the compound in biological systems. To this regard, a greater band gap normally designates a more stable compound with fewer tendencies to participate in chemical reactions [59]. In comparison of the computed CBD and Δ⁹-THC HOMO-LUMO band gap energies, from which it can be inferred that Δ⁹-THC had a larger energy than CBD. Therefore, in chemical environment, CBD can be highly reactive since its electrons can be readily excited compared to Δ⁹-THC. Hence, Δ⁹-THC can be considered more kinetically stable than CBD.

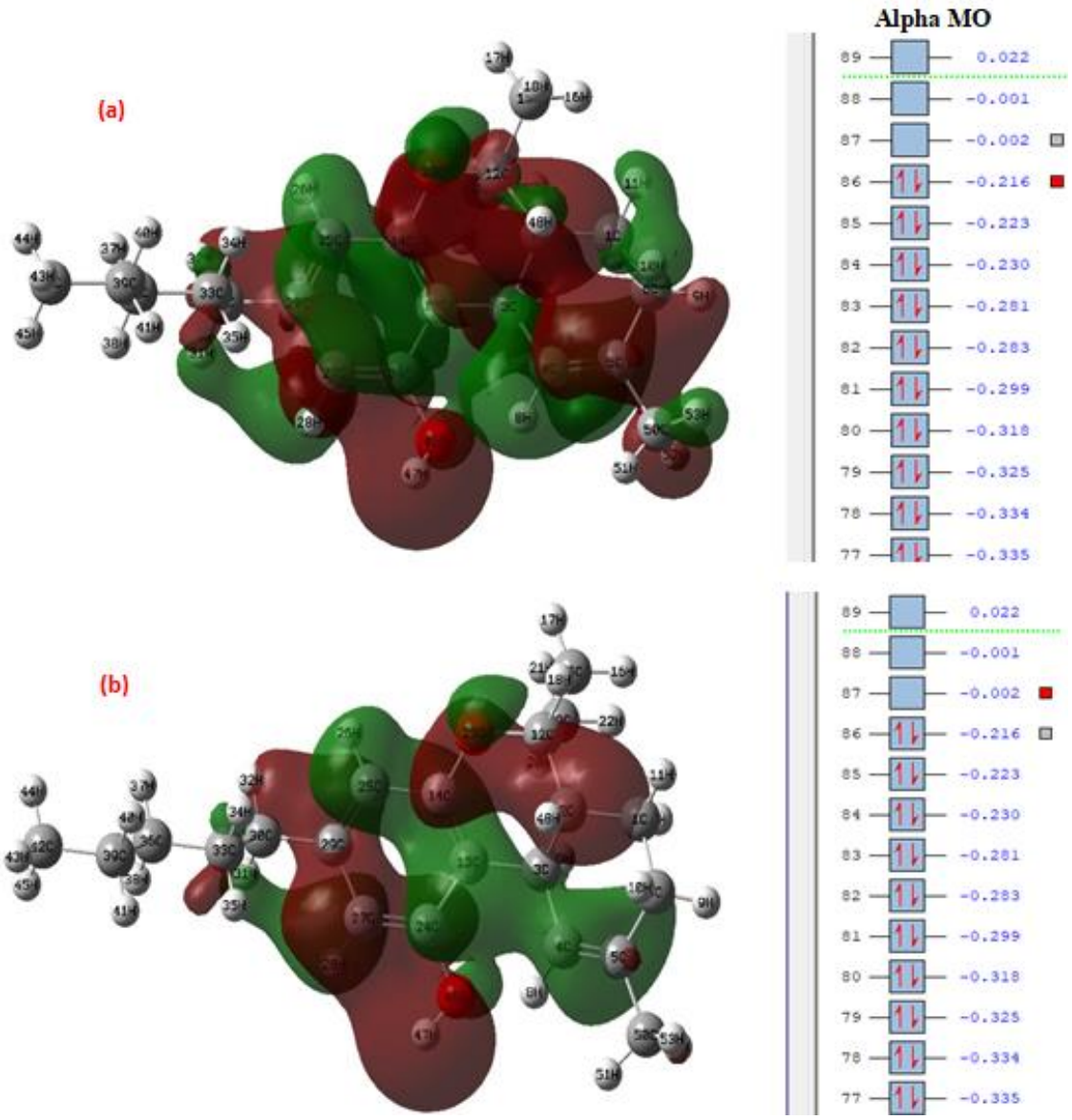

Figure 8. (a) Δ⁹-THC HOMO and (b) Δ⁹-THC LUMO

3.6. Electron density and contour maps

DFT offers an efficient quantum mechanical framework for modeling electron correlation effects in molecular systems [60]. This approach proves particularly effective for characterizing C-H bond formation dynamics, quantifying stabilization energies in molecular complexes and predicting electronic structure properties with experimental accuracy [61]. Computational methods enable the visualization of chemical structures and their specific interaction sites capable of forming hydrogen bonds [60]. These interactions are represented as electrostatic potential maps, which highlight areas with high binding affinity and display the charge distribution across the optimized molecular geometry [53]. The maps provide detailed insights into the electrostatic characteristics of the molecule, revealing favorable regions for hydrogen bonding

based on charge density variations [60]. These considerations are essential for establishing the fundamental framework that describes molecular chemical properties and governs reactivity patterns [61].

The electron density surfaces generated through Gaussian calculations are displayed with color-coded representations, where each hue corresponds to specific electrostatic potential values [62]. These color gradients visually distinguish regions of varying charge distributions, enabling the identification of positive (blue), neutral (green), and negative (red) electrostatic potentials across the molecular surface [53, 63]. This mapping provides an intuitive way to analyze charge polarization and predict sites of potential electrostatic interactions [53, 60]. These density surfaces illustrate the variations in electron distribution bridging the ground state and the lowest excited state by envisioning the computed excited-state electron density [53, 61]. Consequently, the electrostatic potential for Δ⁹-THC and CBD is illustrated in Figure 9 (a) and (b).

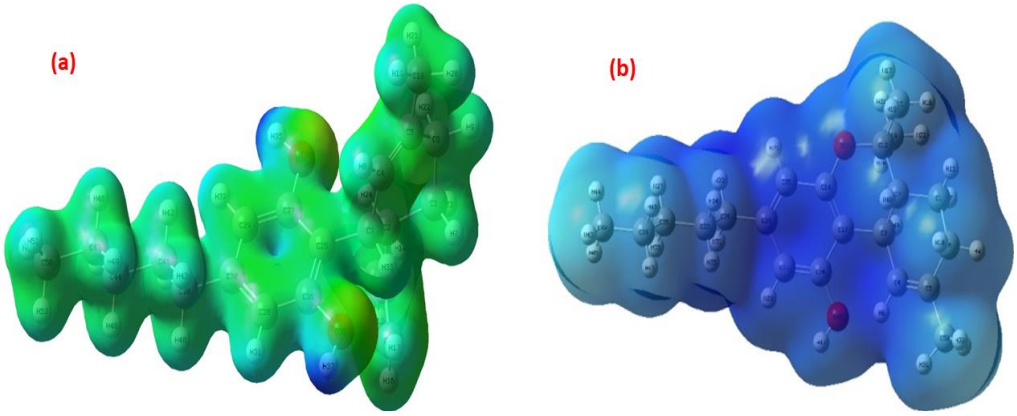

Figure 9. (a) CBD electrostatic potential and (b) Δ⁹-THC electrostatic potential

The blue areas indicate locations with a net increase in electron density upon electronic excitation highlighting regions of positive density difference [62]. On the other hand, the red areas mark locations where the electron density decreases in the excited state, showing a negative difference compared to the ground state [63]. The blue zones indicate areas susceptible to nucleophilic reactivity, while the red zones highlight regions prone to electrophilic interactions [53].

Therefore, for the CBD molecule, electronic charge redistributes from the two hydroxyl groups towards the aromatic ring during transition from the ground to the first excited state. Accordingly, in Δ⁹-THC, the benzene ring adjacent to the hydroxyl group exhibits increased electron density in the excited state, creating a positively enhanced region compared to the ground state configuration. In Δ⁹-THC, electronic charge redistributes from the hydroxyl-attached benzene ring toward both the adjacent aromatic system and alkyl substituents upon excitation to the first excited state. These observed electronic redistribution patterns enabled the creation of the density contour map plots in Figure 10, providing valuable insights into the molecule's charge transfer behavior during electronic excitation [22].

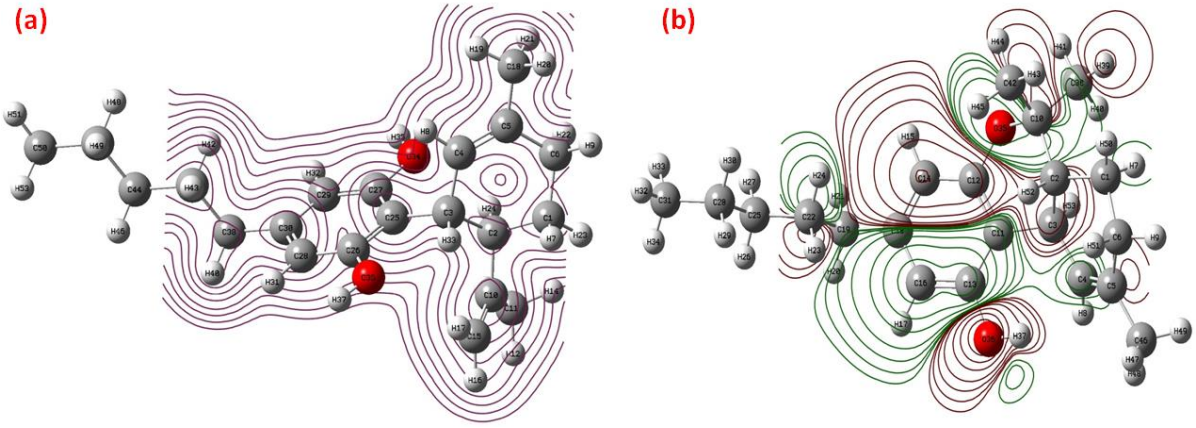

Figure 10. (a) CBD contour map and (b) Δ⁹-THC contour map

3.7. CBD toxicity estimation using qsar in hyperchem 8.0

The relative toxicities of CBD and subsequent radicals were estimated using QSAR incorporated in the HyperChem 8.0 computational program by computing logarithm of octanol-water partition coefficient (Kow) parameters, P, which is mainly a measure of lipophilicity and hydrophobicity of any given chemical compound [64]. In a precise way, lipophilicity values correlate with biological activities like mutagenicity and carcinogenicity that occur in body cells. In this case therefore, computational modelling with QSAR incorporated in HyperChem 8.0 establishes an approach for analyzing pollutants and other persistent environmental toxins [65]. The toxicity indices for CBD and its thermal degradation generated radicals were estimated as listed in table below.

Table 2. QSAR-Derived Partition Coefficients (P) and Log P values for CBD and Its Pyrolytic Derivatives

Compound/ Radical	P	Log P
Cannabidiol	2,570.40	3.41
5-pentylbenzene-1,3-diol	19.50	1.29
1-methyl-4-(prop-1-en-2-yl) cyclohex-1-ene	870.96	2.94
2,6-dihydroxy-4-pentylbenzene-1-yliumyl	14.79	1.17
3-methyl-6-(prop-1-en-2-yl) cyclohex-2-en-1-yliumyl	741.31	2.87

From Table 2, the computed toxicity indices indicate that cannabidiol (CBD), 1-methyl-4-(prop-1-en-2-yl) cyclohex-1-ene, and its corresponding radical, 3-methyl-6-(prop-1-en-2-yl) cyclohex-2-en-1-yliumyl, are potentially the most toxic species. Notably, CBD exhibits a high partition coefficient (P = 2,570.4), suggesting it is significantly more soluble in in octanol than water. In contrast, the radical and derivative molecule showed relatively lower values of 741.31 and 870.96, respectively. This high relative octanol affinity implies that CBD could be highly reactive in lipophilic biological environments. Furthermore, the significant lipophilicity of these compounds is strongly correlated with the ability to penetrate lipid-rich biological barriers, potentially leading to oxidative stress, cellular damage, mutagenesis, and cancer [66, 67]. Consequently, similar adverse health impacts are anticipated from 1-methyl-4-(prop-1-en-2-yl) cyclohex-1-ene and it's radical.

Conversely, 5-pentylbenzene-1,3-diol and 2,6-dihydroxy-4-pentylbenzene-1-ylium exhibited lower partition coefficients (19.50 and 14.79, respectively), indicating lower hydrophobicity and higher aqueous solubility. However, their potential toxicity should not be dismissed, as these compounds may still interact with non-polar cellular components, potentially causing cell alterations and gene mutations.

4. Conclusions

This study has demonstrated that thermal degradation of CBD leads to the formation and release of toxic radicals that have been precursors in the genesis of cell mutation and consequently cancer. With the help of computational tools, the toxicity of these compounds has been discussed in detail. QSAR incorporated in HyperChem 8.0 estimated the toxicity of CBD and its corresponding radicals and found out the species of compounds to be highly reactive to human biosystems where they are prone to attack lipid barrier systems due to their lipophilic nature thereby evoking injurious cell reactions. In this regard, Gaussian 09 computational code has successfully demonstrated the optimized geometries of CBD and Δ^9-THC together with electron density and contour maps which highlighted the electrophilic and nucleophilic site of electron attack for the molecules under study. Just like Δ^9-THC which has been reported in other studies as toxic, CBD thermally degrades into potentially toxic effluents which render it toxic even though it finds application as medication to manage patients suffering from a number of medical conditions including cancer.

Declaration of Conflict of Interests

The authors declare that there is no conflict of interest. They have no known competing financial interests or personal relationships that could have appeared to influence the work reported in this paper.

References

[1.] Omare, M.O., Kibet, J.K., Cherutoi, J.K. and Kengara, F.O. (2021). Current trends in the use of Cannabis sativa: beyond recreational and medicinal applications. *Open Access Library Journal, 8*(6), 1-15. doi: 10.4236/oalib.1107132

[2.] Archie, S.R. and Cucullo, L. (2019). Harmful Effects of Smoking Cannabis: A Cerebrovascular and Neurological Perspective. *Front Pharmacol, 10*, 1481-1481. doi: 10.3389/fphar.2019.01481. https://pubmed.ncbi.nlm.nih.gov/31920665

[3.] Andre, C.M., Hausman, J.-F. and Guerriero, G. (2016). Cannabis sativa: the plant of the thousand and one molecules. *Front Plant Sci, 7*, 19.

[4.] Martinez, A.S., Lanaridi, O., Stagel, K., Halbwirth, H., Schnürch, M. and Bica-Schröder, K. (2023). Extraction techniques for bioactive compounds of cannabis. *Natural Product Reports, 40*(3), 676-717.

[5.] Sharma, P., Murthy, P. and Bharath, M.M. (2012). Chemistry, metabolism, and toxicology of cannabis: clinical implications. *Iran J Psychiatry, 7*(4), 149-56.

[6.] Motamedi, S., Sheibani, V., Rajizadeh, M.A., Esmaeilpour, K. and Sepehri, G. (2019). The effects of co-administration of marijuana and methylphenidate on spatial learning and memory in male rats. *Toxin Reviews*, 1-10. doi: 10.1080/15569543.2019.1633544

[7.] Shrivastava, A., Johnston, M. and Tsuang, M. (2011). Cannabis use and cognitive dysfunction. *Indian J Psychiatry, 53*(3), 187-191. doi: 10.4103/0019-5545.86796. https://pubmed.ncbi.nlm.nih.gov/22135433 https://www.ncbi.nlm.nih.gov/pmc/articles/PMC3221171/

[8.] Hammoud, M., Gorka, S., Rabinak, C., Liberzon, I., Maren, S., Phan, K.L., et al. (2018). S4. Influence of Δ9-Tetrahydrocannabinol (THC) on Fear Extinction Learning and Spontaneous Recovery. *Biological Psychiatry, 83*(9), S348.

[9.] Ford, T.C., Hayley, A.C., Downey, L.A. and Parrott, A.C. (2017). Cannabis: an overview of its adverse acute and chronic effects and its implications. *Current drug abuse reviews, 10*(1), 6-18. doi: 10.2174/1874473710666170712113042

[10.] Sarris, J., Sinclair, J., Karamacoska, D., Davidson, M. and Firth, J. (2020). Medicinal cannabis for psychiatric disorders: a clinically-focused systematic review. *BMC Psychiatry, 20*(1), 24. doi: 10.1186/s12888-019-2409-8

[11.] Stasiłowicz-Krzemień, A., Nogalska, W., Maszewska, Z., Maleszka, M., Dobroń, M., Szary, A., et al. (2024). The use of compounds derived from cannabis sativa in the treatment of epilepsy, painful conditions, and neuropsychiatric and neurodegenerative disorders. *International Journal of Molecular Sciences, 25*(11), 5749.

[12.] Beale, C., Broyd, S.J., Chye, Y., Suo, C., Schira, M., Galettis, P., et al. (2018). Prolonged Cannabidiol Treatment Effects on Hippocampal Subfield Volumes in Current Cannabis Users. *Cannabis Cannabinoid Res, 3*(1), 94-107. doi: 10.1089/can.2017.0047. https://pubmed.ncbi.nlm.nih.gov/29682609

[13.] Duggan, P.J. (2021). The chemistry of cannabis and cannabinoids. *Australian Journal of Chemistry, 74*(6), 369-387.

[14.] Chacon, F.T., Raup-Konsavage, W.M., Vrana, K.E. and Kellogg, J.J. (2022). Secondary terpenes in Cannabis sativa L.: synthesis and synergy. *Biomedicines, 10*(12), 3142.

[15.] Vásconez-González, J., Delgado-Moreira, K., López-Molina, B., Izquierdo-Condoy, J.S., Gámez-Rivera, E. and Ortiz-Prado, E. (2023). Effects of smoking marijuana on the respiratory system: a systematic review. *Substance Abuse, 44*(3), 249-260.

[16.] Khobragade, D.S. (2024). Biomass–An Environmental Concern. *Plant Biomass Derived Materials: Sources, Extractions, and Applications*, 1-22.

[17.] Shehata, S.A., Toraih, E.A., Ismail, E.A., Hagras, A.M., Elmorsy, E. and Fawzy, M.S. (2023). Vaping, environmental toxicants exposure, and lung cancer risk. *Cancers, 15*(18), 4525.

[18.] Meehan-Atrash, J. and Rahman, I. (2021). Cannabis vaping: existing and emerging modalities, chemistry, and pulmonary toxicology. *Chemical research in toxicology, 34*(10), 2169-2179.

[19.] Ng, J.Y., Homayouni, P., Usman, S. and Gomes, Z. (2022). The medical cannabis regulatory framework in Canada: A narrative review. *European Journal of Integrative Medicine, 50*, 102104.

[20.] Pacula, R.L. and Smart, R. (2017). Medical Marijuana and Marijuana Legalization. *Annu Rev Clin Psychol, 13*, 397-419. doi: 10.1146/annurev-clinpsy-032816-045128. https://pubmed.ncbi.nlm.nih.gov/28482686
https://www.ncbi.nlm.nih.gov/pmc/articles/PMC6358421/

[21.] Yu, B., Chen, X., Chen, X. and Yan, H. (2020). Marijuana legalization and historical trends in marijuana use among US residents aged 12–25: results from the 1979–2016 National Survey on drug use and health. *BMC Public Health, 20*(1), 156. doi: 10.1186/s12889-020-8253-4. https://doi.org/10.1186/s12889-020-8253-4

[22.] Mosonik, B.C., Ngari, S.M. and Kibet, J.K. (2019). Molecular Modelling of Selected Combustion By-Products from the Thermal Degradation of Croton megalocarpus Biodiesel. *Open Access Library Journal, 6*(10), 1. doi: 10.4236/oalib.1105840

[23.] Bartocci, E. and Lió, P. (2016). Computational modeling, formal analysis, and tools for systems biology. *PLoS computational biology, 12*(1), e1004591.

How to Cite This Article

Omare, M. O., Kibet, J. K., and Nyabaro O, M., Computational Modeling of Cannabidiol and Δ⁹-Tetrahydrocannabinol Derivatives from the Thermal Degradation of Cannabis sativa, Brilliant Engineering, 1(2026), 41062.
https://doi.org/10.36937/ben.2026.41062